Oil & Gas Science and Technology – Rev. IFP, Vol. 61 (2006), No. 5, pp. 611-630

DOI: 10.2516/ogst:2006002

3-D Land Seismic Surveys: Definition of Geophysical Parameters

A. Chaouch[1] and J.L. Mari[2]

1 Tpa, 12, rue Christophe Colomb, 75008 Paris - France
2 Institut français du pétrole, IFP School, 238, avenue Napoléon Bonaparte, 92505 Rueil-Malmaison - France.
e-mail: abdelkader.chaouch@wanadoo.fr - j-luc.mari@ifp.fr

Résumé — Sismique 3D terrestre : définition des paramètres d'acquisition — Dans la plupart des compagnies pétrolières, les acquisitions sismiques marines 3-D ont augmenté de façon exponentielle entre 1990 et 1996 pour couvrir la majorité de leurs champs. Aujourd'hui, la sismique 3-D est de plus en plus utilisée aussi en terrestre. Des outils spécifiques de pré-planning ont été développés pour déterminer les principales caractéristiques de la future acquisition 3-D tels que le degré de couverture, les distributions d'offsets et d'azimuths, les effets des obstacles de surface, etc. Les études de pré-planning ont pour but de définir les paramètres géophysiques associés aux objectifs géologiques ainsi que les dispositif 3-D à mettre en œuvre et les coûts. Le présent article introduit la terminologie utilisée dans la technologie 3-D et passe en revue les principaux paramètres de cette technologie. La première partie est un glossaire illustré. La seconde partie offre aux géophysiciens d'étude les outils qui permettent d'évaluer rapidement les paramètres géophysiques d'une acquisition 3-D, évaluation basée sur les principes fondamentaux de la propagation des ondes. De plus, elle donne des règles pratiques, souvent présentées sous forme de règles du pouce.

Abstract* — *3-D Land Seismic Surveys: Definition of Geophysical Parameters — *In many major oil companies 3-D surveys increased exponentially from 1990 to 1996 to cover the majority of their offshore fields. Nowadays 3-D surveys are also widely used for onshore fields. Specific pre-planning tools were developed to estimate all characteristics of the future acquisition such as offset, fold and azimuth distributions, effects of surface obstacles, make up shots, etc. The pre-planning aims at defining the geological targets of the 3-D with the associated geophysical parameters, design and costs. This paper introduces the terminology used in 3-D technology. The first part is an illustrated glossary. The methodology described in the second part offers to the 3-D planner to very quickly and safely select the most important geophysical parameters based on wave propagation fundamentals and principles. In addition many practical rules, similar to rules of the thumb, are given.*

NOTATIONS

Receivers

R_y Receiver line spacing
R_x Receiver spacing
R_l Receiver line length
N_r Number of receivers per line
N_{rl} Number of receiver lines
T_r Total number of receivers

Shots

S_x Shot line spacing
S_y Shot spacing
N_s Number of shots per line
T_s Total number of shots
S_l Shot line length
S_d Shot density

Offsets

x Current offset
X_{max} Maximum offset
X_{min} Maximum minimum offset

Fold (F)

IxF In-line fold
CyF Cross-line fold

Survey area

S_a Survey area

Midpoints

T_m Total number of midpoints

Bins

b^2 Bin size (square bin)
T_b Total number of bins

Template

R_l Template length
S_l Template width
$R_l{}^*S_l$ Template size

Tapers

T_{px} In-line taper
T_{py} Cross-line taper
F_x In-line fold build-up
F_y Cross-line fold build-up

Sampling

$\Delta x_{(r,s)}$ Spatial sampling for receivers and shots
Δx_m Spatial sampling in midpoint domain
Δx_o Spatial sampling in common offset plane

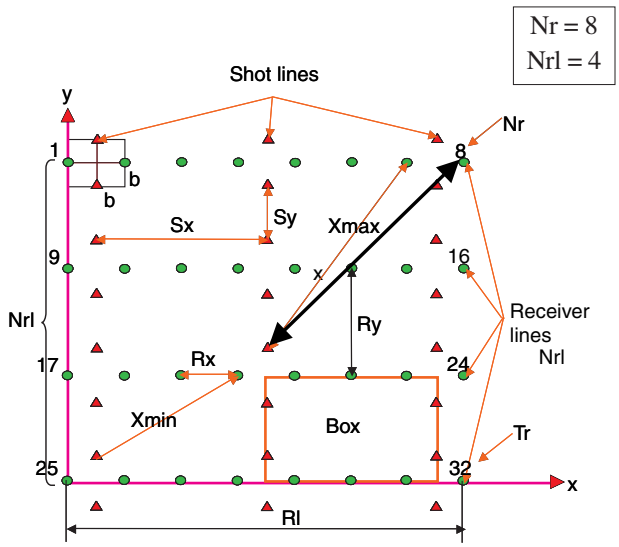

INTRODUCTION

For the last two decades 3-D seismic has progressed significantly. In many major oil companies 3-D surveys increased exponentially from 1990 to 1996 to cover the majority of their offshore fields. Nowadays, acquisition of land 3-D seismic also is developing very quickly. 3-D seismic has reduced many uncertainties in oil and gas exploration and production. The 3-D seismic technology benefits from the development of other techniques such as computers, GPS positioning, increased number of channels in instrument recording, improvements in processing software, etc. 3-D data are now increasingly used for field development and production and not only as an exploration tool. Pre-planning of the 3-D surveys became then a fundamental step to ensure the 3-D data quality will meet structural; stratigraphy and lithology requirements. Pre-planning includes the evaluation of both geophysical and non-geophysical parameters such as environment considerations; health and safety requirements, etc.

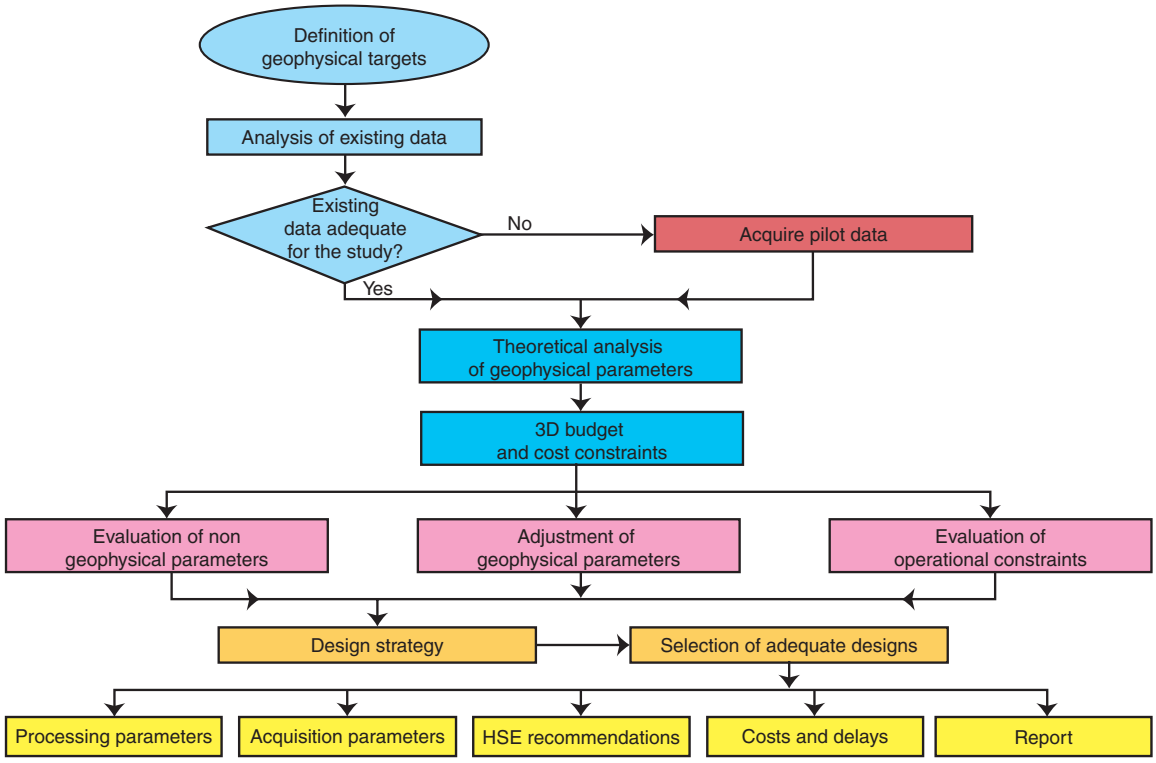

Figure 1

Complete schedule of 3-D evaluation.

Specific pre-planning tools (Cordsen *et al.*, 2000) were developed to estimate all characteristics of the future acquisition such as offset, fold and azimuth distributions, effects of surface obstacles, make up shots, etc. The pre-planning aims at defining the geological targets of the 3-D with the associated geophysical parameters, design and costs. Assessment of the anticipated processing problems is also part of the pre-planning.

Geophysical parameters can be evaluated using wave propagation fundamentals and principles. This evaluation can also use an extensive modelling process based on available seismic data.

Figure 1 describes a complete schedule of the 3-D survey evaluation. However the present article will mainly focus on the methodology based on fundamental considerations of wave propagation. This technique allows a quick evaluation of the planned 3-D, and a reasonable estimation of its budget.

1 3-D TERMINOLOGY

3-D terms may differ from one geophysicist to another. The following section gives the definition of the main terms used in this paper. They are listed in an alphabetic order and illustrated with relevant Figures.

1.1 Box

In an orthogonal design the box *(Fig. 2)* corresponds to the area encompassed by two consecutive receiver lines (spaced R_y) and two consecutive source lines (spaced S_x). Box area is then:

$$S_b = R_y^* S_x$$

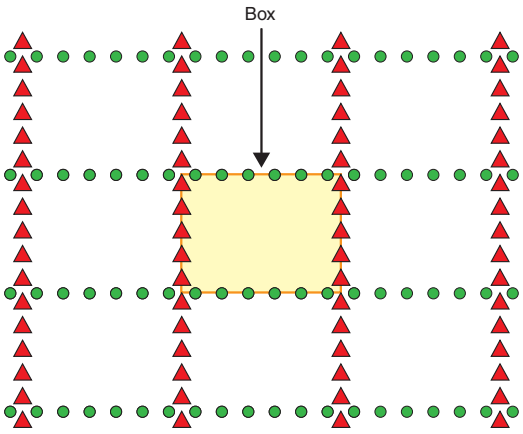

Figure 2

Box.
Receiver lines: horizontal lines. Source lines: vertical lines.

1.2 Directions

Two types of directions *(Fig. 3)* have to be considered:

– **In-line direction**: which is parallel to receiver lines. Sampling in this direction is generally satisfactory.

– **Cross-line direction**: which is orthogonal to receiver lines. Sampling in this direction is generally weak and has to be investigated carefully.

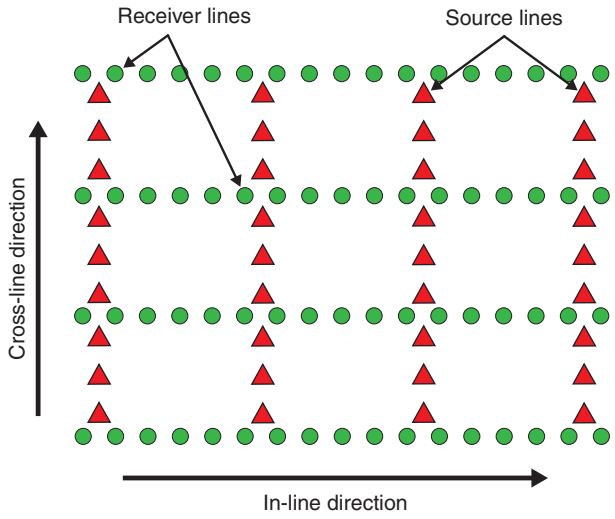

Figure 3

Directions.
Receiver lines: horizontal lines. Source lines: vertical lines.

1.3 Fold of coverage

The 3-D fold *(Fig. 4)* is the number of midpoints *(see 1.4)* that fall into the same bin *(see 1.4)* and that will be stacked. The nominal fold (or *full fold*) of a 3D survey is the fold for the maximum offset. The majority of the bins is filled by the nominal fold.

Due to the reflection technique the fold is not nominal at the edges of a 3-D survey. To build up the full fold in the in-line and cross-line directions, it is necessary to introduce an additional surface area, called halo zone, defined by *fold tapers,* gates in which the fold increases gradually. This halo zone will increase the size of the 3-D area.

– **Run-in**: is the distance necessary to bring the fold from its minimum to its nominal value in the shooting direction.

– **Run-out**: is the distance necessary to bring the fold from its nominal value to its minimum in the shooting direction.

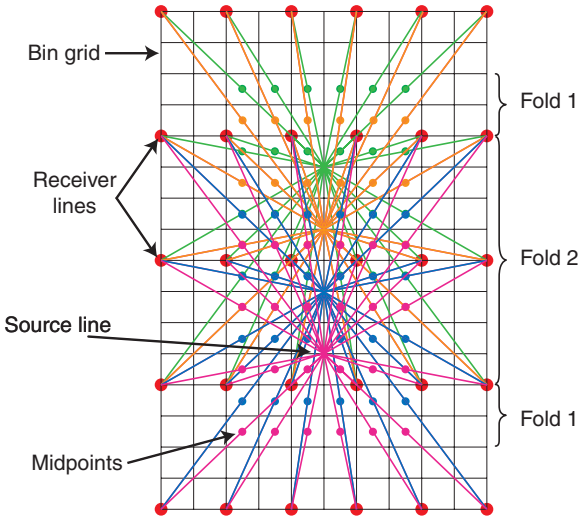

Figure 4

Fold.

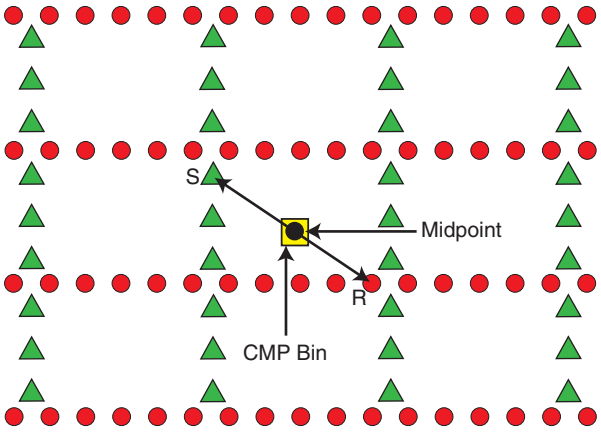

Figure 5

Midpoint.
Receiver lines: horizontal lines. Source lines: vertical lines.

1.4 Midpoint

Midpoint *(Fig. 5)* is a point located exactly in the middle of the source – receiver distance. It is not necessarily located along a receiver line as in 2-D. Instead, midpoints are usually scattered within the survey area. In practice, they rarely form a regular grid.

– **Common mid point (CMP)**: in an horizontal layered medium with constant velocity, common mid point (CMP) is the point located in the middle of different

source-receiver pairs which reflection corresponds to the same subsurface point. It is desirable that source-receiver pairs are different in direction and in offsets.

– **CMP bin**: CMP bin is a square or rectangular area, which contains all midpoints that correspond to the same CMP. Traces that fall in the same bin are stacked. Their number corresponds to the fold of the bin.
– **Bin size**: the bin size corresponds to the length and to the width of the bin. Smallest bin dimensions are equal to half source point interval and half receiver interval *(Sy/2*Rx/2)*.

1.5 Move-Ups

Two types of move-ups *(Fig. 6)* can be considered for 3-D surveys:

– **In-line move-up**: occurs when the template moves up along the survey from its initial position after completion of a salvo of shots.
– **Cross-line move-up**: occurs when the template reaches the edge of the survey area and moves up across the survey to start a new in-line move-up.

1.6 Offsets

Taking into account the configuration of the 3-D template, different offsets can be defined:

– **In-line offset**: is the distance representing half-length of the template in the in-line direction.
– **Cross-line offset**: is the distance representing half-length of the template in the cross-line direction.
– **Maximum offset (X_{max})**: is the distance of half-diagonal of the template.
– **Maximum Minimum offset (X_{min})**: is the length of the diagonal of the box formed by two consecutive receiver lines and two consecutive source lines.

1.7 Patch

A patch is an acquisition technique where source lines are not parallel to receiver lines. If source and receiver lines are orthogonal the spread is called orthogonal (cross spread). If receiver and source lines are not orthogonal the spread is called slant spread. The survey area will be covered by the juxtaposition of patches. Each one represents a unit area obtained by several template moves. Shot points can be inside the template or outside.

1.8 Receiver Line

Receiver line *(Fig. 7)* is a line where receivers are located at a regular distance.

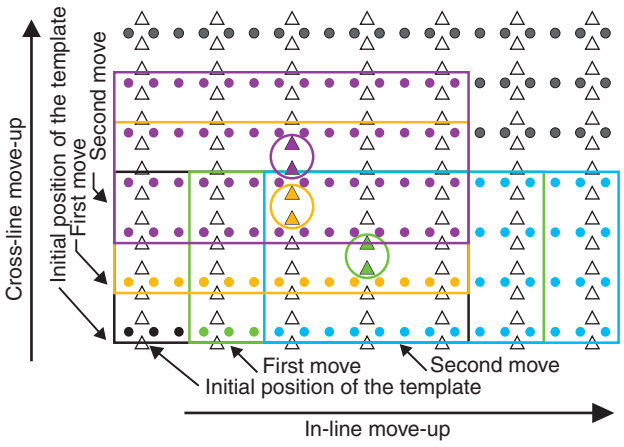

Figure 6

Moves.

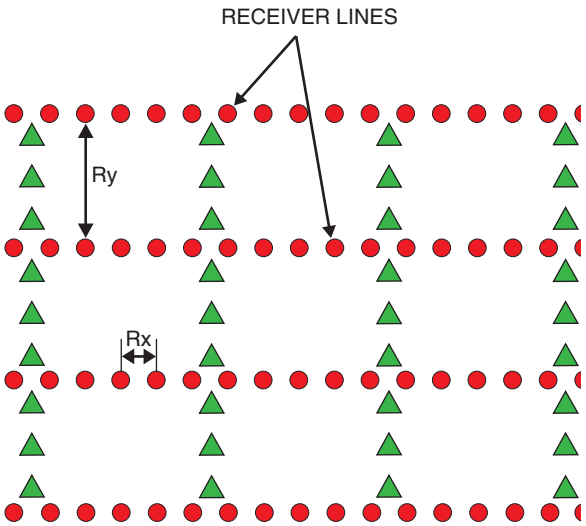

Figure 7

Receiver line: a line along wich receivers are located at a regular distance.
Receiver lines: horizontal lines. Source lines: vertical lines.

In land 3-D surveys receiver lines are kept as straight as possible.

In marine 3-D surveys receiver lines correspond to the towed streamers.

– **Receiver line interval (R_y)**: receiver line interval is the distance between two consecutive receiver lines. It is also called receiver line spacing.

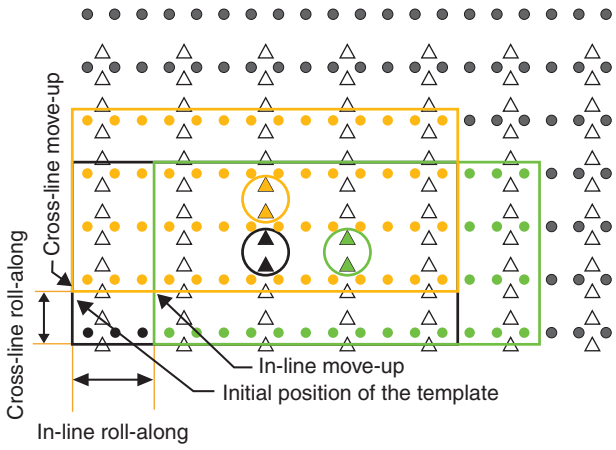

Figure 8

Roll-along.

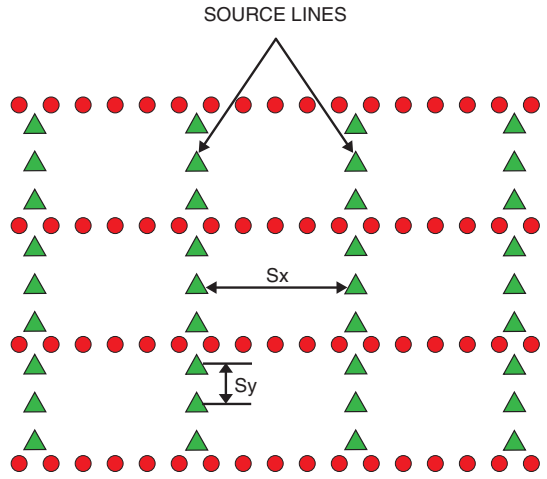

Figure 9

Source ligne: a line where source points are located at a regular distance.
Receiver lines: horizontal lines. Source lines: vertical lines.

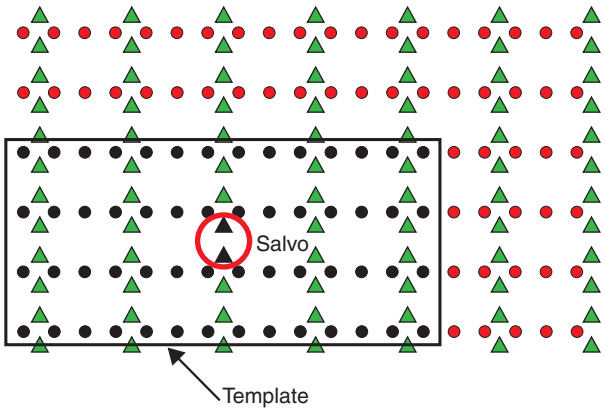

Figure 10

Salvo: shot points within the red circle.
Black rectangle defines the template.

– **Receiver interval** ***(R_x)***: receiver interval is the distance between two consecutive receivers located on the same receiver line. It is also called receiver spacing.
– **Receiver density** ***(R_d)***: receiver density is the number of receivers per surface unit, in general square kilometre *(sq.km)*. Number of receiver lines per kilometre and number of receivers per kilometre determine the receiver density (R_d).

1.9 Roll-Along

Roll-along *(Fig. 8)* is the distance of two consecutive positions of the template. It is a number.

– **In-line roll-along**: corresponds to the in-line move-up of the template and represents the distance between two consecutive positions of the template.
The number of columns of receivers left behind the template is equal to the in-line-roll-along.
– **Cross-line roll-along**: corresponds to the cross-line move up of the template and represents the distance between two consecutive positions of the template.
The number of receiver rows left behind the template is equal to the cross-line-roll-along.

1.10 Source Line

Source line *(Fig. 9)* is a line where source points are located at a regular distance.

In land 3-D surveys source lines can be orthogonal or parallel to receiver lines or have any other direction (slant).

In marine 3-D surveys source lines correspond to the lines followed by airgun arrays.

– **Source line interval** ***(S_x)***: source line interval is the distance between two consecutive source lines. It is also called source line spacing.
– **Source interval** ***(S_y)***: Source interval is the distance between two consecutive source points located on the same source line. It is also called source spacing.
– **Shot density** ***(S_d)***: Shot density is the number of shots per surface unit, in general square kilometre *(sq.km)*. Number of source lines per kilometre and number of sources per kilometre determine the shot density (S_d).

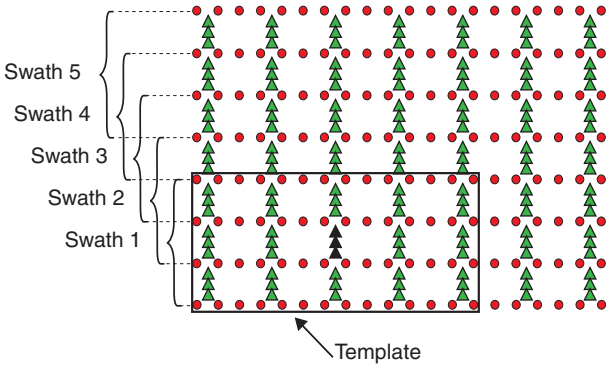

Figure 11

Swath.

Black rectangle defines the template. Black shot points define the salvo.

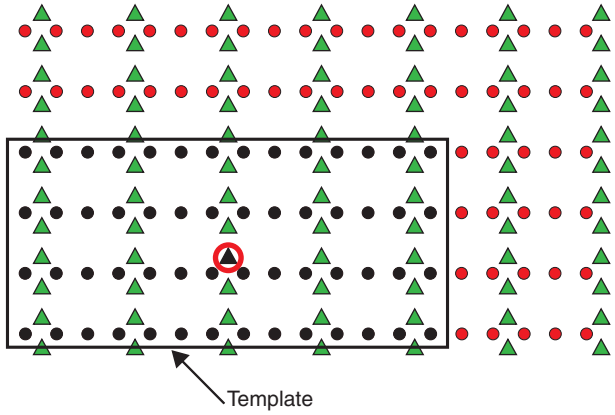

Figure 12

Template: black rectangle.

Actual shot: black shot point. Receiver lines: horizontal lines. Source lines: vertical lines.

1.11 Salvo

A salvo *(Fig. 10)* is the number of fired shots before the template *(see 1.13)* moves up along the survey.

1.12 Swath

When the template *(see 1.13)* moves in one direction and reaches the edge of the survey area, it will generate a swath *(Fig. 11)*. Usually the first move occurs in the in-line direction.

Swath-shooting mode: the swath-shooting mode is an acquisition technique where source lines are parallel to receiver lines.

1.13 Template

All active receivers corresponding to one given shot point corresponds to a template *(Fig. 12)*. These receivers are located on several parallel lines.

1.14 3-D Data

3-D data corresponds to a seismic data volume where CMP traces are located in (*X*, *Y*) co-ordinates independent of the vertical plane of the seismic line.

1.15 3-D Shot Point

A 3-D shot point display *(Fig. 13)* is composed of seismic panels. The number of panels is equal to the number of receiver lines within the template. Shot location can be centered within the template or be at the end or outside the template.

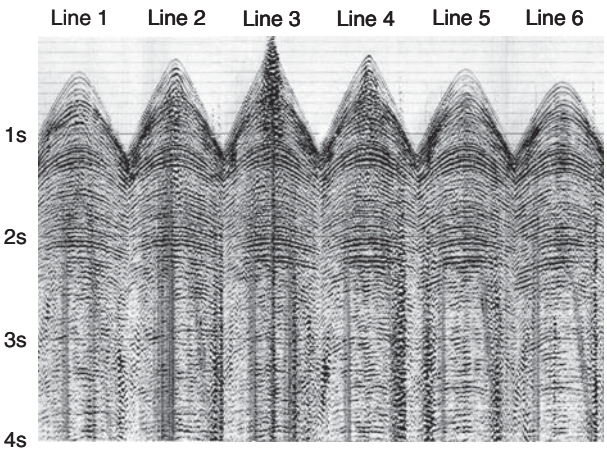

Figure 13

3-D shot point.

6 panels (lines) of 80 receivers each.

The presented shot is composed of 6 regularly spaced receiver lines. Each line has 80 receivers. The shot is centered within the template and is close to line 3.

1.16 3-D Data Volume

3-D data volume is the result of data processing *(Fig. 14)*. It is a migrated volume obtained after sorting the data in CMP bins (binning) and stacking the data.

Data are gathered in (*X*,*Y*,*Z*) coordinates with:

- OX in the in-line direction;
- OY in the cross-line direction;
- OZ in two way time (or depth).

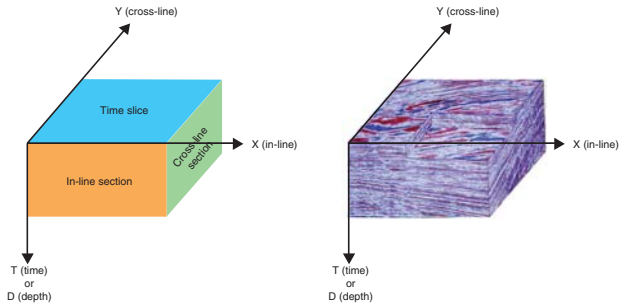

Figure 14

3-D Data volume.

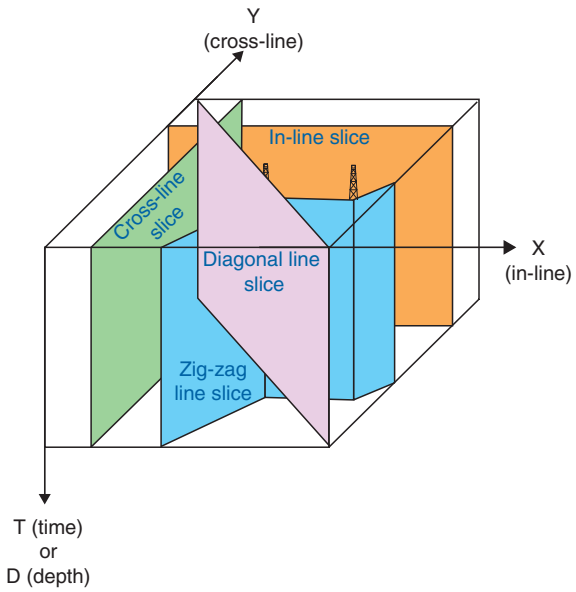

Figure 15

3-D Vertical slices.

In some surveys different volumes can be generated and separately interpreted with:

- near offsets;
- mid offsets;
- far offsets.

1.17 3-D Slices

From the 3-D volume different seismic sections *(Fig. 15)* can be displayed. Some of them are vertical slices, other are horizontal.

- **In-line sections**: are vertical slices parallel to the shooting direction in marine 3D and along receiver lines in land 3D.
- **Cross-line sections**: are vertical slices perpendicular to in-line sections, displayed along the OY axis.
- **Diagonal line sections**: are vertical slices extracted along a given azimuth.
- **Random line sections**: are zigzag vertical slices passing through given points (wells).
- **Time slices**: are horizontal sections extracted at constant times.

2 GEOPHYSICAL PARAMETERS

Geophysical parameters of a 3-D can be gathered into imaging, edge, geometrical and recording parameters. All of them have an impact on the 3-D data quality. However some of them have a great impact on the cost of the survey and have to be adjusted carefully. They correspond mainly to the imaging parameters and are related to fold of coverage, bin size and migration aperture. They are thus related to sampling and aliasing criteria, to resolution and signal enhancement and to migration efficiency:

- Edge parameters include in-line and cross-line tapers.
- Geometrical parameters correspond to offsets and source and receiver lay outs.
- Recording parameters are related to recording length and sampling rate.

2.1 Imaging Parameters

2.1.1 Fold of Coverage

The fold of coverage *(see 1.3)* of a 3-D seismic survey represents the number of traces that are located within a bin and that will be summed. Minimum bin dimensions correspond to half the source interval and half the receiver interval. Each trace is generated in the middle of a source-receiver pair. Source-receiver pairs have different directions. Traces within the bin thus have a range of azimuths and offsets but they correspond to the same subsurface location *(Fig. 16)*.

When summed all traces carry the same signal, which is enhanced as it is in phase. However all traces have different random noise which is out of phase. The summation process decreases the level of noise. Then the fold contributes greatly to the enhancement of the signal to noise (S/N) ratio.

After stacking each bin contains one single trace, whose S/N ratio is multiplied by $\sqrt{F}$ (F being the fold).

Fold vs. *shot density*

The fold is then obtained by the combination of sources and active receivers. As a matter of fact each shot point generates one line of subsurface bins for each active receiver line *(Fig. 17)*.

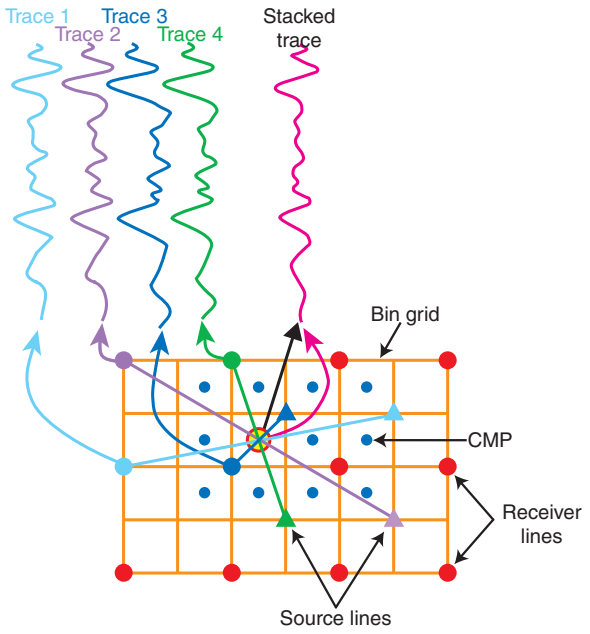

Figure 16

3-D fold.
3-D fold corresponds to the number of traces located within a bin. Traces are generated in the middle of source-receiver pairs, which have different directions.

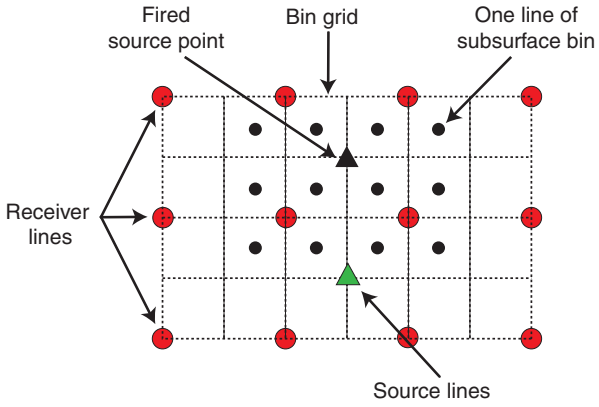

Figure 17

Fold building.
Each shot point generates one line of subsurface bins for each active receiver line. The number of midpoints per subsurface line is equal to the number of receivers.

The number of midpoints per subsurface line is equal to the number of receivers.

Then the total number of midpoints (T_m) is equal to the total number of shots (T_s) multiplied by the total number of receivers (T_r).

$$T_m = T_s * T_r$$

The total number of shots can be expressed by the shot density (S_d) and the survey area (S_a) as:

$$T_s = S_d * S_a$$

The total number of midpoints will be then:

$$T_m = S_d * S_a * T_r$$

The survey area S_a can be expressed by the bin size b^2 (in case of square bin) and the total number of bins (T_b) as:

$$S_a = b^2 * T_b$$

Therefore it follows that:

$$T_m = S_d * b^2 * T_b * T_r$$

In addition, the fold is defined as the number of midpoints in a bin. It can be expressed as:

$$F = T_m / T_b$$

Which is equal to: $F = S_d * b^2 * T_r$ (1)

In this formula S_d is the number of shots per square km and b is in km.

Example of fold calculation:

Consider 4 receiver lines spaced 150 m, with 12 receivers each spaced 50 m and shot lines spaced 100 m with shot spacing of 50 m orthogonal to receiver lines.

The nominal fold is 6.

Nominal fold vs. *in-line and cross-line fold*

The nominal fold can also be expressed as the product of in-line fold *(IxF)* by cross-line fold *(CyF)*

$$F = IxF * CyF$$

The in-line fold is similar to 2-D line fold:

$$IxF = R_l / (2 * S_x) = N_r * R_x / (2 * S_x) = (N_r / 2) * (R_x / S_x)$$

Similarly the cross-line fold is defined as:

$$CyF = (N_{rl} / 2)*(Sy/Ry) * (\text{Salvo} / (\text{Cross-line roll along}))$$

Then the nominal fold can also be expressed by:

$$F = [(\text{Salvo}) / S_xR_y(\text{Cross-line Roll along})] *[(R_x/2)(S_y/2)] [(N_r)(N_{rl})] \quad (2)$$

To evaluate the 3-D fold, some practical rules were defined at the start up of the 3-D surveys. The 3-D fold was generally selected between one third (1/3) and two third (2/3) of the best quality 2-D fold in the survey area.

One third corresponded to areas where the S/N ratio is very good and where static problems are limited. Two thirds corresponded to difficult areas and for comparable results between 2-D and 3-D data geophysicists used 3-D fold as equal to half the 2-D fold.

With new recording instruments and the increase of the number of traces on the field, the 3-D fold is no more an issue. It can be as high as for 2-D or even higher if necessary.

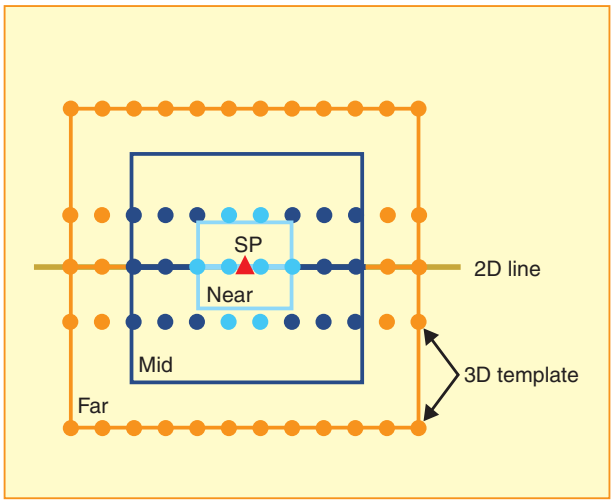

Figure 18

Offset distribution within a 2-D line and a 3-D template.
For 2-D line offsets are regularly distributed. For 3-D template contribution of offsets within a bin is different for near, mid and far offset classes.

Offset distribution

As shown in Figure 18 the fold of 2-D surveys has a regular offset distribution. It contains an equal number of near, mid and far offsets. Each class represents one third (1/3) of the offset number.

To the contrary, for 3-D surveys the contribution of each class of offset is different; with a high percentage of far offsets (about 57%), a small percentage of mid offsets (about 33%) and a very small percentage of near offsets (about 10%).

So the high contribution of far offsets will improve the suppression of multiples, whereas the small amount of near offsets will reduce the noise associated with this class of offsets such as ground roll, air blast, source generated noise, etc. This will result in an improvement in the S/N ratio.

2.1.2 Bin Size

The bin size will affect the lateral resolution of the survey and its frequency content.

Resolution and bin size

Resolution is defined as the ability of a seismic method to distinguish two events of the subsurface that are close to each other. Lateral resolution (also called horizontal resolution) corresponds to the direction parallel to the seismic measurement plane. It is related to the Fresnel zone.

The Fresnel zone is defined as the subsurface area, which reflects energy that arrives at the earth's surface within a time delay equal to half the dominant period (T/2). In this case ray paths of reflected waves differ by less than half a wavelength. Commonly accepted value is one-fourth the signal wavelength *(λ/4)*.

Then a recorded reflection at the surface is not coming from a subsurface point, but from a disk shape area, which dimension is equal to the Fresnel zone.

The radius of the Fresnel zone is given by:

$$R_f = (V/2)(t_0/f_{dom})^{1/2} \quad (3)$$

This shows that high frequencies give better resolution than low frequencies and resolution deteriorates with depth and with increasing velocities.

Migration technique drastically improves resolution as seen in Table 1 (Yilmaz, 1987).

TABLE 1

Migration drastically improves lateral resolution

	s	m/s	Hz	m ($R_f=(V/2)(t_0/f_{dom})^{1/2}$)	m ($R_f=\lambda/2=V/2f_{dom}$)
Depth ↓	Two way travel time (t0)	Rms Velocity increases with depth	Frequency decreases with depth	Radius of Fresnel Zone R, before migration	Radius of Fresnel Zone R, after migration
	1.0	2000	55	134	18
	1.5	2500	50	216	25
	2.0	3000	40	335	38
	2.5	3500	35	468	50
	3.0	4000	30	632	67
	3.5	4500	25	842	90
	4.0	5000	20	1118	125

The 3-D migration is a major factor that drastically improves the 3-D imaging compared with 2-D data as the energy is by far better focused.

In 3-D processing, out of the plane events are restored to their correct subsurface location and become additional energy.

As a matter of fact the migration can be considered as a downward continuation of receivers from the surface to the reflector making the Fresnel zone smaller and smaller. The 3-D migration will shorten the radius of the Fresnel zone in all directions *(Fig. 19)* improving drastically the resolution.

Bin size must be equal to the lateral resolution after migration. This value is equal to half the dominant wavelength λ_{dom} associated with the dominant frequency f_{dom}.

$$Bin\ size = {}^1/_2\ \lambda_{dom} \quad (4)$$

Spatial sampling and bin size

Spatial sampling is a common operation in seismic acquisition. The recorded samples must allow the reconstruction of

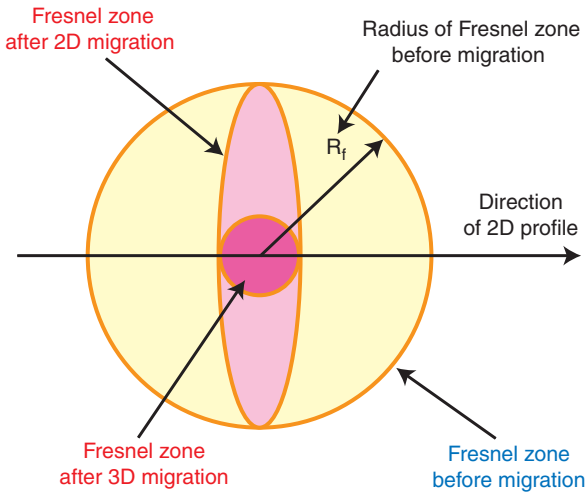

Figure 19

Lateral resolution.
3-D Migration shortens the radius of Fresnel zone in all directions improving the resolution.

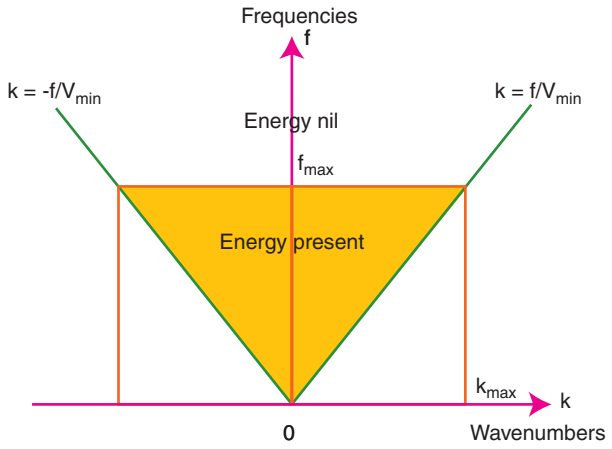

Figure 20

Nyquist wavenumber.
In the *(f,k)* plane there is a maximum wavenumber $|k_{max}|$ such that the energy is nil for frequency superior to f_{max} (Vermeer, 1998).

the original signal without ambiguity. A proper sampling is given by Nyquist condition (or Shannon theorem), which states that two samples per period are minimum to reconstruct a discrete signal. Then sampling interval is:

$$\Delta t \leq T/2 \text{ or } \Delta t \leq {}^1/_2 f_{max}$$

According to Gijs Vermeer, in the *(f,k)* plane there is a maximum wave number $|k|_{max}$ such that the energy is nil for frequency superior to f_{max} and there is a minimum velocity V_{min} *(Fig. 20)*.

The spatial sampling for shots and receivers is thus:

$$\Delta x_{(r,s)} \leq V_{min} / 2f_{max} \quad (5)$$

Whereas the spatial sampling in the midpoint domain is:

$$\Delta x_m \leq V_{min} / 4f_{max} \quad (6)$$

For dipping events (with dip θ), the above formulae become:

$$\Delta x_{(r,s)} \leq V_{min} / 2f_{max} \sin\theta \quad (7)$$

$$\Delta x_m \leq V_{min} / 4f_{max} \sin\theta \quad (8)$$

These formulae give the maximum-recorded frequency and wavenumbers and no alias occurs.

However, if V_{min} is very small or F_{max} is very high the above formulae lead to very small Δx, which is very difficult to implement. Then it is common in acquisition to accept some kind of signal that is aliased such as ground roll with low velocity or noise with high frequency.

Diffractions and bin size

Diffractions are useful for migration and should be sampled correctly. The sampling formula is (Liner and Underwood, 1999):

$$\Delta x \leq V_{rms} / 4f_{max} \sin\varphi \quad (9)$$

Where φ is the take-off angle from the diffraction point.

It is considered that if the take-off angle is equal to 30° the corresponding wave front carries 95% of the diffracted energy.

Then the above formula gives an antialias sampling value equal to:

$$\Delta x \leq V_{rms} / 2f_{max} \quad (10)$$

Sampling paradox

Compared to the surface diagram (shot-receiver coordinate system) the subsurface diagram (midpoint-offset coordinate system) shows "that, the distance between adjacent traces in the CMP (Common Midpoint Panel) is twice the distance between receivers. Also, in the COP (Common Offset panel) the distance between adjacent traces is twice as large as the distance between adjacent CMPs. For proper sampling in (x_s,x_r) this leads to under sampling in (x_m,x_o)" (Vermeer, 1998).

Practical rules

In summary, bin size must be selected as the minimum value of the following three formulae:

$$\text{Bin size} = {}^1/_2 \lambda_{dom}$$
$$\Delta x_{(r,s)} \leq V_{min} / 2f_{max} \sin\theta$$
$$\Delta x \leq V_{rms} / 2f_{max}$$

In addition the sampling paradox must be considered either by square sampling in shots and receivers or by implementing additional shots or by two dimensional interpolation procedure.

2.1.3 Migration Aperture

Migration aperture is defined as a fringe that must be added around the subsurface target area in order to correctly migrate

dipping events and correctly focus diffracted energy located at the edge of the target area. Migration aperture is then related to the two aspects of migration techniques: moving dipping events to their true subsurface locations and collapsing diffractions. The external limit of the migration aperture corresponds to the full fold area.

Migration aperture and migration displacements

Migration restores the dipping reflector to its true position with three effects: shortening the reflector, increasing reflector dip and moving reflector in the up-dip direction with horizontal and vertical displacement.

Horizontal and vertical displacements are given by the following formulae (Chun and Jacewitz, 1981):

$$D_h = (V^2 * t * \tan \theta_s)/4 \quad (11)$$

θ_s being the dip angle on the time section:

$$D_v = t\{ 1 - [1 - (V^2 * \tan^2 \theta_s)/4]^{1/2}\} \quad (12)$$

$$\tan \theta_s = D_v / D_h$$

The migrated angle θ_m is given by:

$$\tan\theta_m = \tan\theta_s / [1 - (V^2 * \tan^2 \theta_s)/4]^{1/2} \quad (13)$$

Table 2 gives a threshold of migration displacements and indicates that:

- dips after migration are higher than dips on stack,
- steep dips are more displaced than smaller dips,
- the deeper the reflector the larger the displacements,
- high velocities generate high displacements.

TABLE 2

Deeper the reflector larger the displacements and higher the velocity larger the displacements

t(s)	V(m/s)	D_h(m)	D_v(s)	θ_s(ms/tr)	θ_m(ms/tr)
1	2500	625	0.134	10	11.5
2	3000	1800	0.400	10	12.5
3	3500	3675	0.858	10	14.0
4	4000	6400	1.600	10	16.7
5	4500	10125	2.820	10	23.0

In conclusion

Events visible on stack sections are not only located in this section. They can represent events located laterally or deeper than the seismic line. Thus, to take into account migration effects, dimensions of the target area must be extended by at least values of the horizontal displacement. In the same way recording length must be long enough to take into account vertical migration displacement.

Migration aperture and diffractions

The following considerations discussed in 2D are also available in 3D. Diffractions are generated by subsurface features whose dimensions are smaller than the incident seismic signal such as pinch-out, erosional surface, abrupt lithology changes, reefs, flanks of salt dome, faults, etc.

In the *(x,z)* plane each discontinuity will generate a circular diffracted wavefront which will be recorded at the surface at different offsets $x_1, x_2,.. x_n$ at times $t_1,t_2,.. t_n$.

In the (x,t) plane, couples (x_1,t_1), (x_2,t_2), etc. give a diffraction hyperbola in the stacked data. The apex of this hyperbola indicates the diffractor point and its equation is:

$$t = 2 (z^2 + x^2)^{1/2} / V_{rms}$$

In theory the hyperbola extends to infinite time and distance. However in practice, for the migration, the diffraction hyperbola will be truncated to a spatial extent within which the migration process will collapse the energy to the apex of the hyperbola. This extent is called migration aperture and its width determines the accuracy of the migration. It is accepted to limit the extension of the hyperbola to 95% of the seismic migration energy. This corresponds to a take-off angle from the apex of 30° as shown in Figure 21a.

Figure 21b gives the value of the migration aperture as:

$$M_a = z * \tan\theta$$

with θ minimum equal to 30°, this gives:

$$M_a = z * \tan 30^\circ = 0.577 * z$$
$$M_a \approx 0.6 * z = 0.6 * (Vt_0 / 2) \quad (14)$$

where V is the average velocity and t_0 is the zero-offset time.

In case of dipping event the migration aperture is:

$$M_a = z * \tan\alpha$$

It then follows that:

$$M_a = (Vt_0 / 2) * \tan\alpha \quad (15)$$

where α is the maximum geological dip.

Migration aperture and migration algorithms

The migration algorithms give another limitation of the migration aperture. These algorithms, in general, take into account dips of 45 to 60 degrees and too steep dips are not well imaged after migration. Dips can then be limited to these values.

Migration aperture and velocity

(Yilmaz, 1987) shows that migration aperture increases with velocity as indicated in the above formulae and the deeper the geological targets the higher the migration aperture.

Practical rules

Migration aperture will be:

$$M_a \approx 0.6 * z = 0.6 * (Vt_0 / 2)$$

if the maximum geological dip is less than 30°.

If this angle is higher than 30° the migration aperture will be:

$$M_a = z * \tan\alpha = (Vt_0 / 2) * \tan\alpha$$

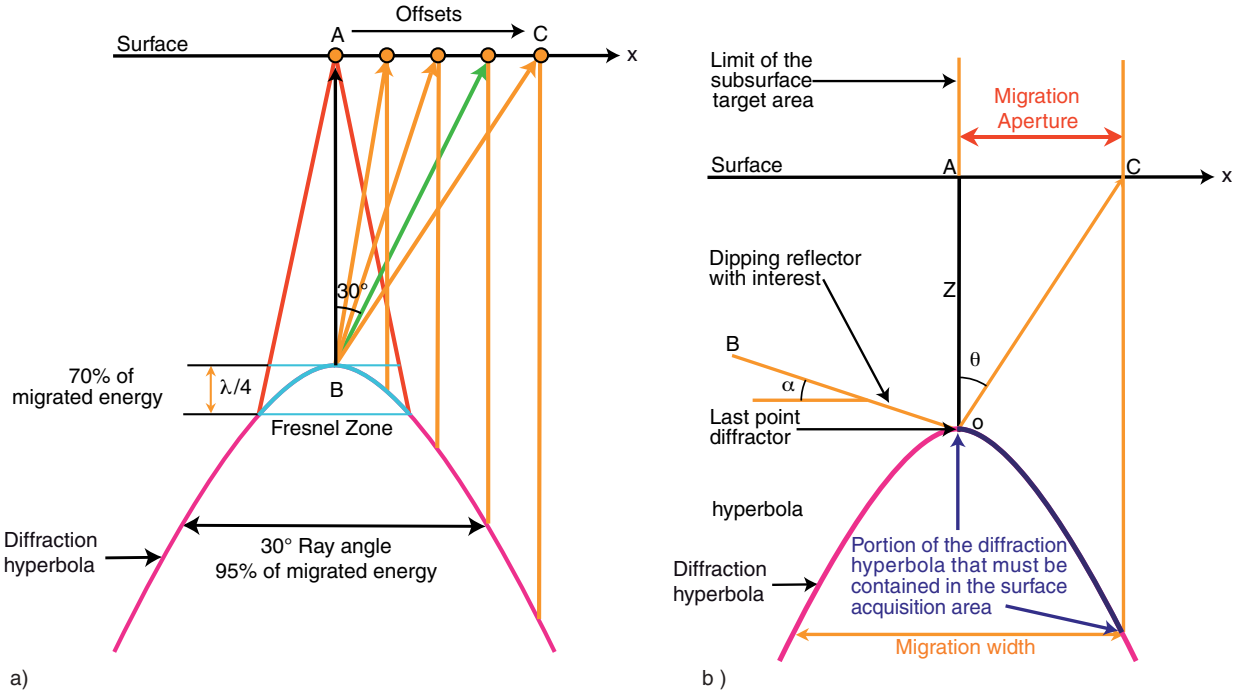

Figure 21

Migration aperture.
a): 95% of the seismic migration energy is contained within a take-off angle of 30°.
b): Migration aperture value $M_a = z*tan\theta$.

In addition the maximum dip can be limited by the dip limit of migration algorithms.

Migration aperture and cost

Let us consider a geological target area of 20 × 10 = 200 sq.km.

The above formulae indicate that the migration aperture to be added to this area is proportional to the depth of the reflector of interest and to the maximum geological dip.

Table 3 gives a threshold for the influence of the migration aperture on the cost.

TABLE 3

Depth of geological target in m	Maximum geological dip					
	30°		45°		60°	
	Migration aperture M_a in m	Additional cost in %	Migration aperture M_a in m	Additional cost in %	Migration aperture M_a in m	Additional cost in %
1000	600	18,7	1000	32,0	1730	57,8
2000	1200	38,8	2000	68,0	3460	227,7
3000	1800	60,5	3000	208	5200	310,0

2.2 Edge Parameters

Edge parameters are essentially related to the fold distribution around the full fold area *(Fig. 22a and b)*. In this area the fold is not nominal. It is the halo zone. Instead it has to be managed in order to bring it from a minimum value to its full value. The distance to be added to the full fold area is called fold taper. In 3-D acquisition two types of tapers have to be considered: the in-line taper corresponding to the receiver lay out direction and the cross-line taper corresponding to the orthogonal direction.

2.2.1 In-Line Taper

For the in-line taper the minimum value of the fold is usually taken equal to one. However it could be higher in case of cost savings.

The distance Tx of the in-line taper is:

$$Tx = (IxF/2 - 0.5) * Sx \quad (16)$$

It is usually more practical to calculate the in-line fold build-up F_x in terms of source line interval with the expression:

$$F_x = (S_x * F) / T_x \quad (17)$$

where:

F = nominal fold

IxF = in-line fold

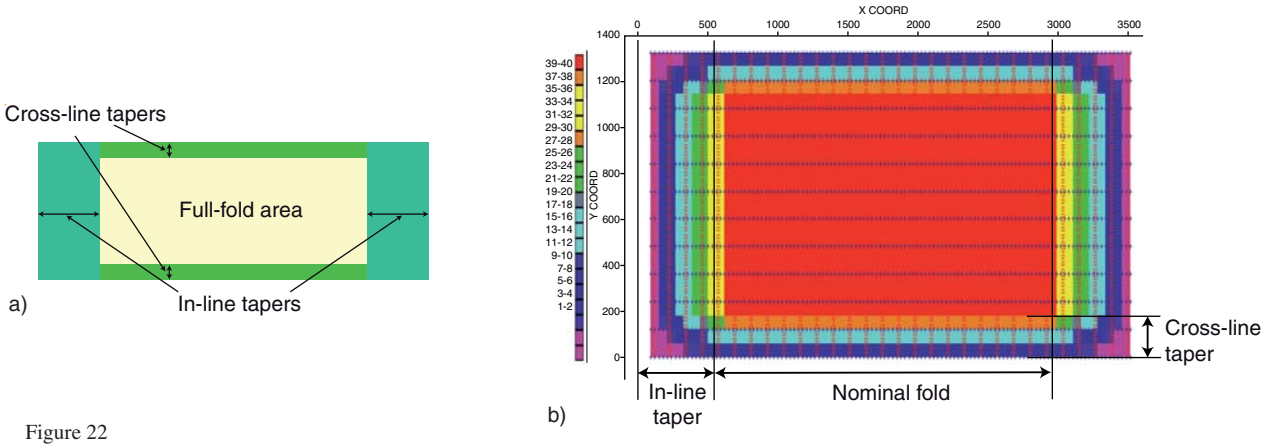

Figure 22

Fold tapers.
a) definition.
b) example.

S_x = shot line spacing
T_x = in-line taper in meters
F_x = in-line taper in number of source line spacing intervals

2.2.2 Cross-Line Taper

The cross line taper depends on the template configuration.

The distance T_x of this taper is:

$$T_y = (CyF/2 - 0.5) * R_y \quad (18)$$

and the cross-line fold build-up F_y in terms of receiver line interval is given by:

$$F_y = (R_y * F) / T_y \quad (19)$$

where:

F = nominal fold
CyF = cross-line fold
R_y = receiver line spacing
T_y = cross-line taper in meters
F_y = cross-line taper in number of receiver line spacing intervals

Fold taper considerations

Folder taper represents then an additional area to be added around the full fold area. It is needed for operational aspects. It can greatly increase the size of the survey area. This makes small 3-D surveys very expensive.

Practical rules

For flat layers, the in-line fold taper can be taken approximately 20% of the maximum offset (X_{max}).

$$T_x \approx 20\% * X_{max} \quad (20)$$

Fold tapers and cost

Let us consider the same geological target as above with 20 × 10 = 200 sq.km. Let us take:

$$T_x \approx 20\% * X_{max}$$

and

$$T_y \approx 0.7 * T_x$$

The following Table 4 gives a threshold for the influence of fold tapers on the 3-D cost.

TABLE 4

Maximum offset X_{max} in m	In-line taper T_x in m	Cross-line taper T_y in m	Additional cost in %
1000	200	140	5%
2000	400	280	10%
3000	600	420	15%
4000	800	560	20%

The additional cost related to fold tapers could be limited by selecting designs where the fold build-up is faster. It is also possible to relax the fold at the extreme edge of the survey area in case compromises have to be taken (reduced budget, border problems, etc.).

2.3 Conclusions of the Imaging and Edge Parameters

Imaging and edge parameters lead to the conclusion that for the planning of 3-D seismic surveys three areas must be considered to ensure an optimum quality of the results. Each area has its own purpose and a bad estimation of one area may deteriorate drastically the quality of the 3-D.

The first area (blue) is defined during the interpretation and corresponds to the subsurface target area that must be fully migrated. Correctly imaging this area is the main objective of the 3-D as it is the area that will be interpreted after complete processing. It is called *subsurface full fold fully migrated area* (area 1 on *Fig. 23*).

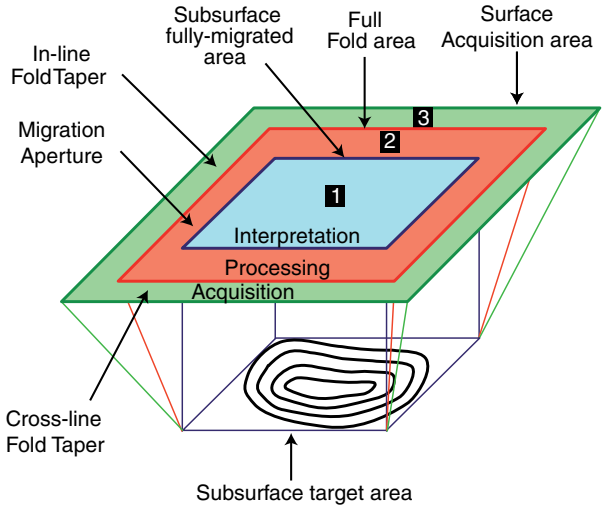

Figure 23

3-D seismis survey areas.
For 3-D seismic surveys three areas must be considered.
1) Subsurface Full Fold Fully Migrated area; 2) Full fold area; 3) Surface Acquisition area.

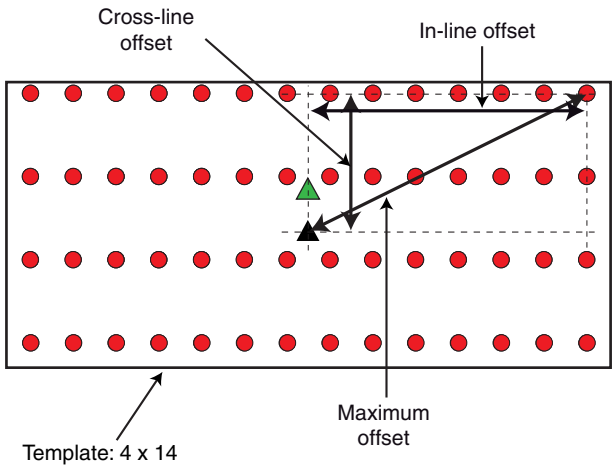

Figure 24

Maximum offset.
Definition for orthogonal design.

The second area (red) is the area that will impact the processing. Its extension will influence the migration software to correctly collapse the energy lying in this area to the edge of the fully migrated area (area 1). Its width represents the migration aperture and the fold within it is nominal. It is called *full fold area* (area 2 on *Fig. 23*).

The last surface (green) that encompasses the previous ones is needed for operational requirements. It corresponds to the fold build-up around the full fold area. The external limit of this area corresponds to the survey area, which is the *surface acquisition area* (area 3 on *Fig. 23*).

2.4 Geometrical Parameters

2.4.1 Maximum Offset: X_{max}

Maximum offset X_{max} *(Fig. 24)* corresponds to the distance between the actual shot and the farthest receiver in the template. It is approximately equal to half the diagonal of the template:

$$X_{max} = (X_{cross}^2 + X_{in}^2)^{1/2}$$

where:

X_{max} = maximum offset;

X_{cross} = Distance between the actual shot and the farthest receiver line in the cross-line direction;

X_{in} = Distance between the actual shot and the farthest receiver in the in-line direction.

Many factors influence the selection of the maximum offset such as: depth of geological target, mute function, NMO correction, NMO stretch, direct arrival, multiple discrimination, available equipment, etc.

Maximum offset and deepest target depth

Maximum offset must be large enough to image the primary geological target of the 3-D.

$$X_{max} \geq Z$$

For flat layers X_{max} can be equal to the depth Z of this target.

Maximum offset and mute function

The mute function is defined during processing in order to eliminate the noise generated at the beginning of each trace. The mute function can be seen on previous seismic surveys. This function will limit the maximum offset to avoid acquiring data that will be eliminated during processing.

$$X_{max} = X_{mute}$$

Maximum offset and NMO correction

Normal move out (NMO) correction is used in processing to align reflections seen on different traces before stack. NMO corrections are applied to data sorted in CMP bin gathers. Previously, the data recorded in 3D shot point gathers are pre processed in order to separate the wanted waves from the unwanted waves. The unwanted waves are direct waves, refracted waves and surface waves. For that purpose, different wave separation methods such as f-k filtering, matrix filtering, polarisation filtering (Mari *et al.*, 1997) can be used. Several methods can be combined to increase the efficiency of wave separation and to enhance the signal to noise ratio. Furthermore the pre-processing includes multiple suppression. Multiple attenuation can be obtained by methods based on velocity discrimination between primaries and multiples in both the f-k and t-k domains, by methods based on predictive deconvolution or by methods based on wave extrapolations using the wave equation. However, nothing being perfect, the pre-processed CMP bin gathers can be corrupted by residues of unwanted waves and multiples. Figure 25 shows a synthetic CMP bin gather before and after NMO correction.

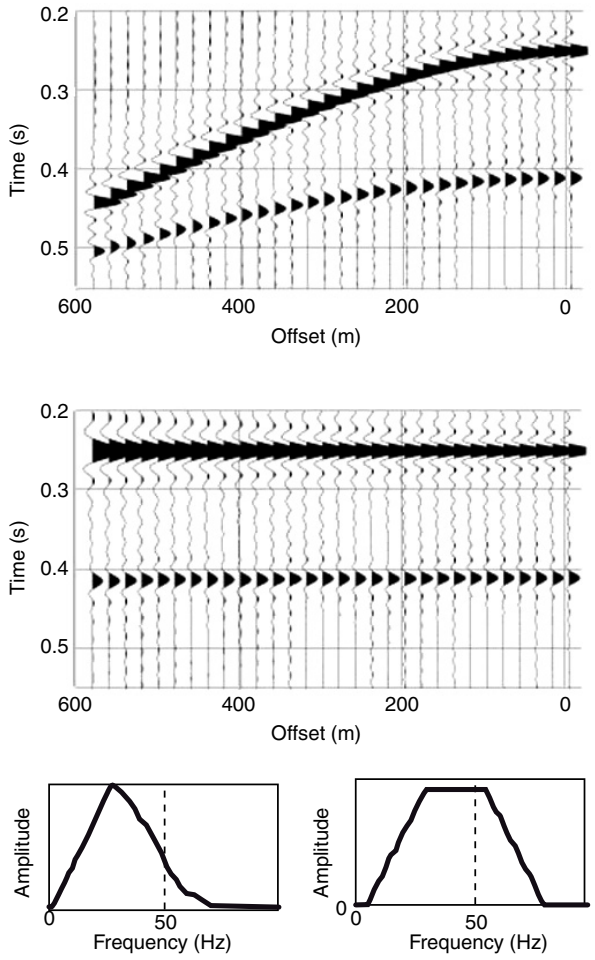

Figure 25

Stretching effect.
Synthetic CMP bin gather. Upper part: CMP before NMO correction. Middle part: CMP after NMO correction (note the stretching effect).
Lower part: amplitude spectra after NMO correction for a near offset trace (on the right) and for a far offset trace (on the left).

For a horizontally stratified medium, the travel time equation t_x for a wave reflected on a layer associated with the normal incident travel time t_0 is:

$$t_X^2 = t_0^2 + X^2 / V_{RMS}^2 + C_2X^4 + C_3X^6 + ...$$

where:

X is the source – receiver offset,

t_0 is the normal incident travel time,

V_{RMS} is the rms velocity,

C_2, C_3,... are complicated functions that depend on interval velocities, layer thickness and coefficients of anisotropy.

By making the small spread approximation (maximum offset smaller than the maximum target depth) the travel time equation can be written as follows:

$$t_X^2 = t_0^2 + X^2 / V_{NMO}^2 \quad (21)$$

The *t-x* curve associated with the reflected wave is close to a hyperbolic curve given by the previous equation. The velocity V_{NMO} required for NMO correction for a horizontally stratified medium is equal to the rms velocity. A NMO correction Δt_{NMO} is computed for each trace at offset X and subtracted from the recorded time t_X. This operation transforms each t_X to an equivalent normal incident travel time t_0. The NMO correction Δt_{NMO} is equal to $t_X - t_0$ ($\Delta t_{NMO} = t_X - t_0$). As the velocity usually increases with time, the NMO hyperbola becomes flatter and flatter at longer offsets. Thus, for any offset, time difference between two hyperbolae is smaller than the corresponding time difference at zero-offset. To fill this difference the wavelet is stretched for NMO corrected traces (see *Fig. 25*, middle part). Because of the stretched waveform at large offsets, stacking the NMO- corrected traces will severely damage the shallow events. This problem can be solved by muting the stretched zones in the CMP bin gathers.

Assuming that $\Delta t_{NMO}^2 << 2.t_0 .\Delta t_{NMO}$, the NMO correction Δt_{NMO} can be approximated by the following equation:

$$\Delta t_{NMO} \approx X^2 / (2.t_0.V_{NMO}^2) \quad (22)$$

NMO correction introduces NMO stretching marked by frequency distortion of the wavelets. After NMO correction, a wavelet with a dominant period T is stretched and becomes a wavelet with a dominant period T_{STR} larger than T. $\Delta T = T_{STR} - T$ is change in period. For a wavelet of dominant period T, the approximated NMO correction (Δt_{NMO}) equation can be used to quantify the change in period ΔT:

$$X^2 / (2.V_{NMO}^2) \approx t_0 .\Delta t_{NMO} = (t_0 + T).(\Delta t_{NMO} - \Delta T)$$

Assuming that $T << t_0$, it follows that $\Delta t_{NMO} / t_0 = \Delta T/T = (T_{STR} - T)/T = \Delta f/f$, where f is the dominant frequency associated with the dominant period T and Δf the change in frequency.

Stretching is quantified by a stretching factor α (expressed in percentage):

$$\alpha = \Delta f/f = \Delta t_{NMO} / t_0 \quad (23)$$

Figure 25 (lower part) shows the change in frequency, loss of the high frequency components of the amplitude spectrum, introduced by the stretching. The stretching factor is used to define automatic mute function $X_{mute}(t_0)$ as:

$$X_{mute}^2 = 2.t_0.\Delta t_{NMO}.V_{NMO}^2 = 2.\alpha .t_0^2.V_{NMO}^2$$

$$X_{mute} = \sqrt{2\alpha}.t_0.V_{NMO} \quad (24)$$

Maximum offset X_{max} and consequently maximum Δt_{NMO} must be large enough to get accurate velocity analysis and to get multiple discrimination, especially if the multiple filtering is based on velocity discrimination between primaries and multiples. X_{max} must be less than the offset X_{mute} where NMO stretch becomes unacceptable. A stretching factor of about 15% is currently used. This leads us to define X_{max} as:

$$X_{max} < X_{mute} \approx \text{depth of geological target.}$$

The offset selection is usually done by automatic mute function at the processing.

Practical rules

X_{max} can be selected as the minimum of offsets required to correctly image the deepest marker. X_{max} should also be less than the offset where NMO stretch becomes unacceptable. Finally it will allow correctly AVO analysis.

2.4.2 Maximum Minimum Offset: X_{min}

In an orthogonal design many source-receiver pairs have their midpoint at the central bin of the box.

The shortest offset in that bin is the largest minimum offset of the whole survey called X_{min}.

It corresponds to the diagonal of the box.

If R_y and S_x are the dimensions of the box *(Figs. 2 and 26)*, X_{min} in orthogonal design, in brick design and in zig-zag design is given by:

$$X_{min} = (R_y^2 + S_x^2)^{1/2} \quad (25)$$

In order to avoid duplicate offsets, source lines are offset by half the receiver spacing *(Fig. 26b)*

X_{min} is then given by:

$$X_{min} = ((R_y - S_y)^2 + (S_x - R_x)^2)^{1/2} \quad (26)$$

Maximum minimum offset and shallowest target depth

The shallowest reflector must be sampled correctly to be processed adequately. At least a fold of 4 to 5 is necessary.

For flat layers maximum minimum offset must be less than the depth of the shallowest geological target.

$$X_{min} < Z_{sh}$$

Maximum minimum offset and critical refraction angle

The critical refraction angle will limit the minimum offset and X_{min} should respect the refraction criterion.

In order to sample the velocity of the shallowest refractor at least three measurements are necessary.

X_{min} should be less than the offset of the critical refraction angle. This angle is about 35°.

$$X_c = 2 * Z * tani_c$$

$$X_c = 2 * Z * tan35^\circ$$

$$X_c = 1.4 * Z_{sh}$$

$$X_{min} < X_c$$

This value allows only single fold.

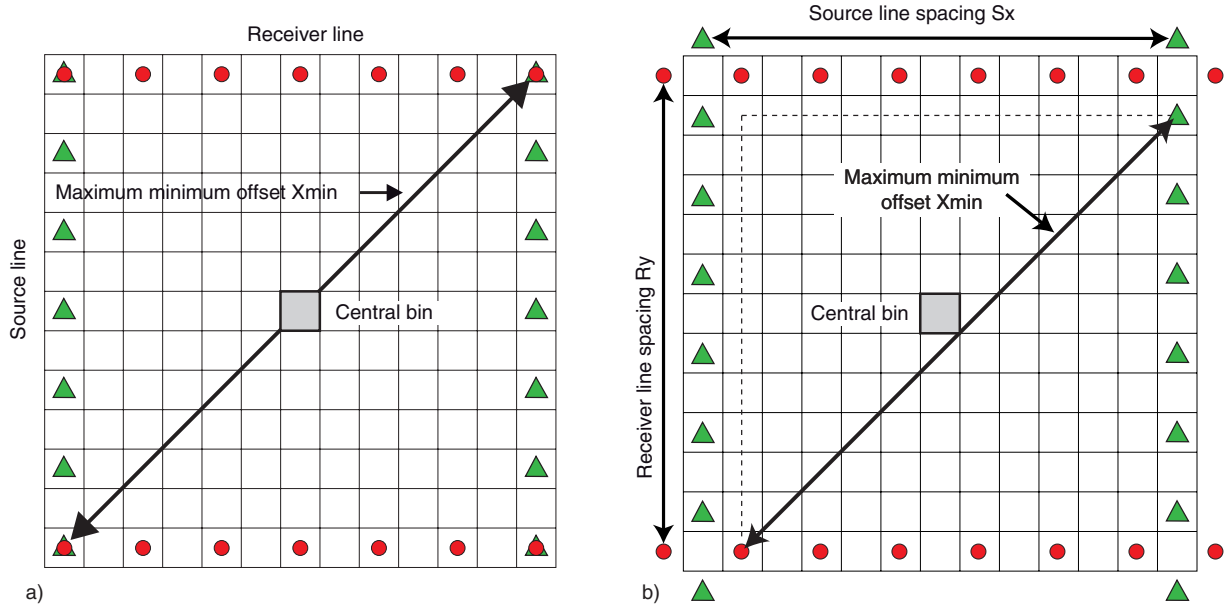

Figure 26

X_{min} definition.
a) in case of the shot points are not offset.
b) in case of the shot points are offset.

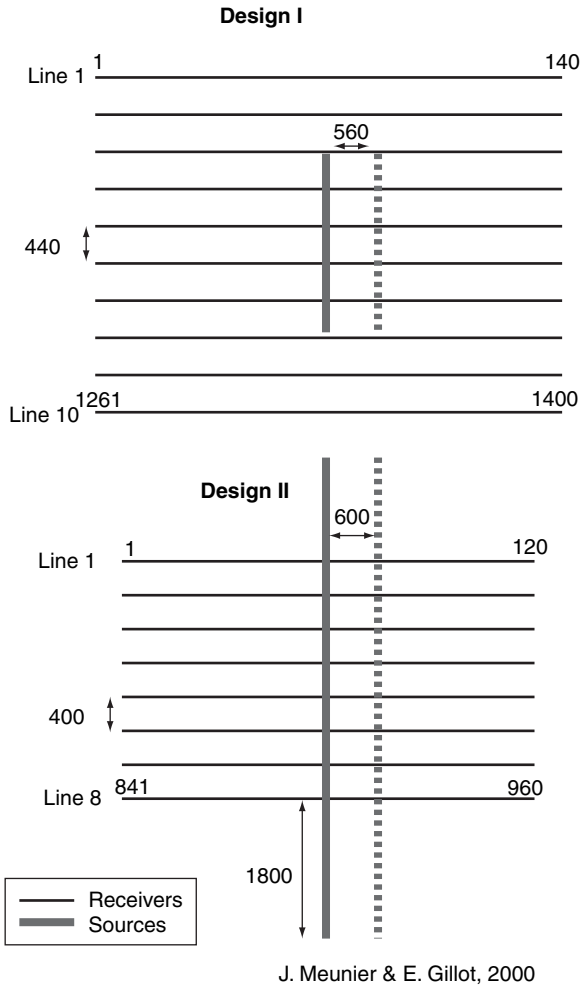

		Design I	Design II
Receiver spacing (m)	Rx	40	50
Shot spacing (m)	Sx	560	600
Number of receivers / line	Nr	140	120
In line fold	IxF	5	5
Receiver line spacing (m)	Ry	440	400
Shot spacing (m)	Sy	40	50
Number of receiver lines	Nrl	10	8
Number of shots / template	Salvo	55	128
Swath overlap	SO	5	0
Cross line fold	CyF	5	8
Fold	F	25	40
Bin size	b^2	20 x 20	25 x 25
Shot density	Sd	44.64	66.67

Figure 27

Example of orthogonal designs.

Practical rules

To be in the safe side X_{min} should be taken equal to 1 to 1.2 Z_{sh}.

2.5 Recording Parameters

Recording parameters are essentially related to recording length and sampling rate.

2.5.1 Recording Length

Recording length should be selected taking into account the two way time (TWT) of the deepest horizon of interest, the migration aperture time to collapse diffractions generated by deepest formation, static shifts and processing requirements.

Recording length has to be adjusted to its necessary value to avoid a useless increase of the duration of the survey.

2.5.2 Sampling Rate

Sampling rate must be 2 ms or less, in order to record a Nyquist frequency as high as possible. In this case the highest frequency will be equal to:

$$f_{max} = 1 / 2\Delta t = 1 / (2 * 2.10^{-3}) = 250 \text{ Hz}$$

Sampling rate has a direct effect on the amount of data to be recorded and then on the number of tapes to be used.

As an example, let us consider a template of 5 receiver lines with 120 receivers each, (5 × 120) and a recording length of 5 seconds.

For a sampling rate of 2 ms, each shot will generate:

Nsamples = $(5.10^3) / (2.10^{-3}) * 120 * 5 = 15.10^8$ samples

Practical rules

Recording length can be chosen longer than needed, and sampling rate chosen as small as possible as tapes are not

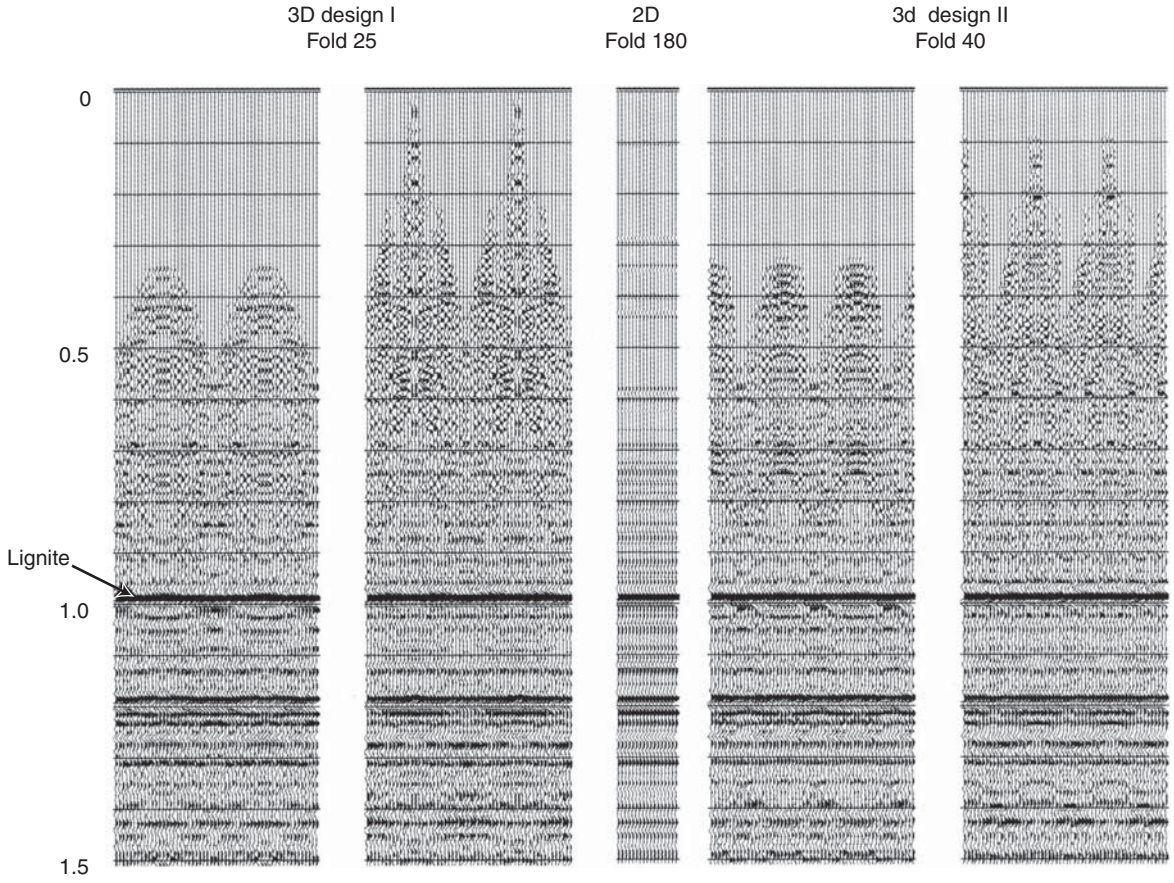

Figure 28

Comparison between 2-D and 3-D stack simulations (Meunier and Gillot, 2000).

very expensive. However the duration of the survey and its cost must be taken into consideration.

CONCLUSION

The methodology described here allows the 3-D planner to very quickly and safely select the most important geophysical parameters. However many inputs in the proposed formulae can be difficult to derive from available data. In addition many practical rules are similar to rules of the thumb.

In spite of these comments the methodology is a good approach to give quickly a reliable budget and a time frame of the planned 3-D survey. This can be done within two weeks after available data collection.

The methodology must be completed by an adjustment of geophysical parameters that leads necessarily to the adjustment, and usually a decrease, of the cost. This adjustment will be carried out using seismic modelling. In comparison with the first technique the duration of such modelling can last two to three months after available data gathering.

The 3-D survey evaluation must be completed by the elaboration of acceptable designs and by the selection of the most operational one. Many designs can be associated with the previous defined geophysical parameters. Some of them can be considered as standard such as orthogonal, brick, zig-zag, star and circular. Such definition was used for the 1999 EAGE 3-D seismic design workshop (Hornman and Vermeer, 2000). For this workshop five specialists in the design of 3-D surveys were invited to recommend survey design parameters based on a common case study. The proposed designs are orthogonal (Meunier and Gillot, 2000; Lansley, 2000; Monk and Yates, 2000), slant (Musser, 2000) and double zig-zag (Galbraith, 2000). An overview of 3-D design solutions is given by Vermeer and Hornman (2000). In this workshop three specialists out of five have selected the orthogonal design. Figure 27 shows the orthogonal designs and the geophysical parameters proposed by Meunier and Gillot (2000).

Additional information is required to select the final design. Usually the design that reduces the footprint is adopted. Footprint can be seen computing offset limited fold maps. To evaluate the footprint effects, simulations with available data are performed. Simulations are also used to quantify the influence of the geophysical parameters. Figure 28 shows a comparison between 2-D stack simulation (using a single 2-D CMP) and 3-D stack simulation from the 3-D designs presented Figure 27.

In this particular case, the 2-D CMP is in fact a shot point. The simulation validity is restricted to horizontal reflections (above all targets). In these conditions, it provides an evaluation of the image degradation in the bin with the largest minimum offset (X_{min} = 684 m for design 1, X_{min} = 686 m for design 2). The example shows that the degradation is not marginal. However, the authors expect that a thorough velocity and static analysis applied to a true bin gather will significantly improve the seismic image (Meunier and Gillot, 2000).

The previous example shows the benefits of seismic modelling to optimise the choice of 3-D design. Modelling and designs will be topics of a future paper.

ACKNOWLEDGEMENTS

We are grateful to Jean-Luc Piazza *(TOTAL)*, for providing useful information and very interesting comments. We thank Dominique Chapellier *(Institut Géophysique de Lausanne)* and Laurent Cuilhe *(BEICIP)* for very useful discussions on various occasions.

REFERENCES

Cordsen, A., Galbraith, M. and Peirce, J. (2000) Planning land 3-D seismic surveys – SEG Series n09 – Bob A. Hardage Ed.

Yilmaz, O. (1987) Seismic data processing, SEG, Tulsa.

Vermeer, G.J.O. (1998) 3-D symmetric sampling, *Geophysics,* **63**, 1629-1647.

Liner, C.L. and Underwood, W.D. (1999) 3-D seismic survey design for linear v(z) media, *Geophysics,* **64**, 486-493.

Chun, J.H. and Jacewitz, C. (1981) Fundamentals of frequency – domain migration, *Geophysics,* **46**, 717-732.

Mari, J.L., Glangeaud, F. and Coppens, F. (1997) Signal processing for geologists and geophysicists, Technip Ed.

Hornman, K. and Vermeer, G.J.O. (2000) Introduction to a 3D design problem, First break, **18**, 5, 161.

Meunier, J. and Gillot, E. (2000) 3D seismic survey design: a solution, First break, **18**, 5, 176-179.

Lansley, M. (2000) 3D seismic survey design: a solution, First break, **18**, 5, 162-166.

Monk, D. and Yates, M. (2000) 3D seismic survey design: a solution, First break, **18**, 5, 180-183

Musser, J.A. (2000) 3D seismic survey design: a solution, First break, **18**, 5, 166- 171.

Galbraith, M. (2000) 3D seismic survey design: a solution, First break, **18**, 5, 171-176.

Vermeer, G.J.O. and Hornman, K. (2000) Introduction to a 3D design problem, First break, **18**, 5, 184-185.

Final Manuscript receveid in March 2006